Electrical and dielectric properties of the $Bi_4Sr_3Ca_3Cu_4O_x$ (4:3:3:4) glassy semiconductor

K. K. Som and B. K. Chaudhuri
Department of Solid State Physics, Indian Association for the Cultivation of Science, Calcutta 700 032, India
(Received 8 June 1989; revised manuscript received 10 October 1989)

The first measurements, in the temperature range of 80–420 K, are reported for the dc and ac conductivities and dielectric constant of the $Bi_4Sr_3Ca_3Cu_4O_x$ (4:3:3:4) oxide glass which, when properly annealed, becomes a superconductor with $T_c \sim 80$ K. The experimental electrical-conductivity data have been analyzed with reference to various theoretical models based on a polaron-hopping conduction mechanism. Hopping of the polaron seems to be adiabatic in nature. At low temperature the dc conductivity data for this glass qualitatively obey Mott's $T^{-1/4}$ law. The analysis shows that the correlated-barrier-hopping model is the most appropriate one for explaining the ac conductivity of the (4:3:3:4) glass. This model quantitatively predicts the temperature dependence of both the ac conductivity and its frequency exponent. The other models such as the quantum-mechanical tunneling model appear to be consistent with the behavior of low-temperature ac conductivity, but fail to interpret the observed temperature dependence of the frequency exponent. Similarly, the overlapping-large-polaron tunneling model qualitatively explains the temperature dependence of ac conductivity at low temperature, but fails in the high-temperature regime. This (4:3:3:4) glassy semiconductor is also found to show Debye-type dielectric dispersion characterized by a relaxation frequency.

I. INTRODUCTION

The semiconducting glasses containing transition-metal oxides (TMO) are very important because of their interesting physical properties as well as for their applications in switching and memory devices,[1–4] cathode-ray-tube materials,[5] ferrites,[6] etc. Recently $Y_1Ba_2Cu_3O_x$ (1:2:3), $Bi_4Sr_3Ca_3Cu_4O_x$ (4:3:3:4) glasses have been prepared containing the transition-metal ions.[7–10] These glasses are very interesting because they could be converted into high-temperature oxide superconductors by properly annealing in air or in oxygen atmosphere.[7–10] This is a new technique for making high-T_c superconducting oxide materials from a "glass-ceramic route." These results prompted us to the detailed characterizations of the (4:3:3:4) glassy semiconductors.

It is well known that the transition-metal oxides, viz., V_2O_5, Fe_2O_3, CuO, etc., when heated with suitable glass formers like Bi_2O_3, P_2O_5, GeO_2, etc., form semiconducting oxide glasses.[11–22] The semiconducting properties of the vanadate glasses have been most extensively studied[11–18] compared to other transition-metal oxide glasses such as iron- and copper-containing glasses.[19–21,23] The electron-phonon interaction in these glassy semiconductors is strong enough to form small polarons[13,14] and the dc electrical conduction occurs by the hopping of small polarons between the transition-metal ions of the two different valence states.[11–18] The ac conductivity of these glasses at low temperature and low frequency showed almost a linear frequency dependence.[15,19–22]

In the above-mentioned oxide glasses, low-valency transition-metal ions (TMI) are created as a consequence of the loss of oxygen from the melt. In these cases the deficiency of the oxygen plays a dominant role in the conduction mechanism of the TMO glasses. This is very similar to the case of recently discovered high-temperature oxide superconductors (like Y-Ba-Cu-O, Bi-Sr-Ca-Cu-O, Tl-Ba-Ca-Cu-O, etc., systems),[24–28] where oxygen deficiency plays a vital role in making these ceramic oxides superconductors, metallic, semiconductors, or insulators.[29]

As mentioned, the glass sample $Bi_4Sr_3Ca_3Cu_4O_x$ (4:3:3:4) prepared by a quick quenching technique[7,8,10] was found to be semiconducting and it could be made superconducting by properly annealing the glass[7–10] as observed from the studies of electrical conductivity and magnetic susceptibility[9] of the corresponding annealed sample.

In this paper the temperature-dependence electrical (both ac and dc) and dielectric properties of the (4:3:3:4) glassy semiconductor have been fitted with the existing theoretical models[13,14,30–33] to find the most suitable model for this glass with the aim of understanding the conduction mechanism in these interesting glass systems. Our organization of the paper is as follows.

In Sec. II we have discussed in short the experimental procedure and technique which have already been published elsewhere[11,12,18,19] while studying several other oxide glasses. Section III deals with the experimental results and discussion. The various theoretical models used to fit the experimental data for the ac and dc conductivities have also been shortly discussed in this section before drawing the final conclusion in Sec. IV.

II. EXPERIMENT

The (4:3:3:4) glass has been prepared by a quick quenching technique similar to our earlier work.[7,8] Ap-

propriate amounts of reagent-grade Bi_2O_3, $CaCO_3$, CuO (E. Merck, Germany), and $SrCO_3$ (Aldrich, U.S.A.), all of purity $\gtrsim 99.99\%$, were well mixed in an agate morter. The mixture was melted in a platinum crucible at a temperature of 1200 °C for 2 h in air with occasional stirring to make the melt homogeneous. The melt was then poured quickly onto an ice cooled stainless steel block and immediately pressed by another similar block. The amorphous nature of the glass was checked by x-ray diffraction (Philips, PW-1050/51) and scanning electron microscopic (Hitachi, Japan) studies.[7,8] The x-ray diffraction patterns of the (4:3:3:4) glass and the annealed (4:3:3:4) sample are shown in Fig. 1. It is observed that with the increase of annealing temperature above T_g the crystallinity and conductivity grows. Similar results have also been reported by Chung and Mackenzie[34] for the vanadate glasses. It should be mentioned here that the (4:3:3:4) glass annealed at higher temperature ($T > T_g$) shows higher conductivity, and the sample annealed at 825 °C for 24 h in air becomes superconducting.[7–9]

Differential-thermal-analysis (DTA) and thermogravimetric (TGA) analysis were done with a Shimadzu DT 30 (Japan) thermal analyzer with a heating rate of 20 °C/min. Chemical analysis using atomic absorption spectroscopy (Perkin Elmer, Model 2380) were done to determine the copper concentration in the (4:3:3:4) glass.

The methods of measuring dc and frequency-dependent ac conductivities, and dielectric constants of the semiconducting glasses have already been discussed earlier.[19,22] The samples for the electrical measurements were annealed at about 100 °C below the glass transition temperature T_g. For electrical and dielectric studies samples of the diameter ≈ 1 cm were cut and polished properly. dc conductivity of the sample in the temperature range of 80–420 K was measured with a Keithley 614 electrometer. However, the limitation in the temperature range utilized was the experimental difficulty of measuring currents of less than 10^{-14} A with the equipments available. The Ohmic contacts were checked by drawing I-V characteristics. The dielectric constant and ac conductivity measurements were carried out with a General Radio (Model GR 1615A) capacitance bridge which measures equivalent parallel capacitance and conductance of the sample in a three terminal arrangement. Gold was used as electrode material. An evacuated chamber was employed as a sample cell which was inserted in the cryogenic unit for low-temperature measurements. Temperature measurements were made with an accuracy of ± 0.5 K using copper-Constantan thermocouple.

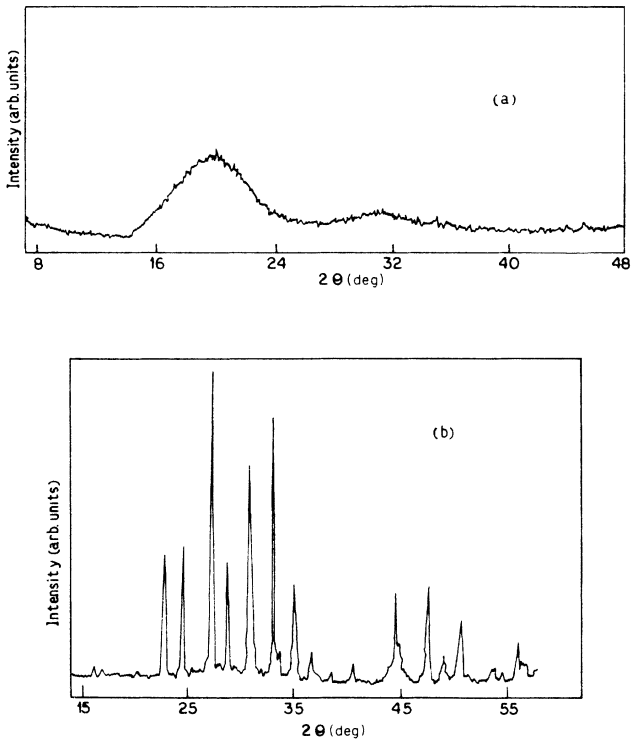

FIG. 1. X-ray diffractograms of (a) the (4:3:3:4) glass and (b) superconductors.

III. RESULTS AND DISCUSSION

A. DTA and chemical analysis

The DTA and TGA curves are shown in Fig. 2. An endothermic peak due to glass transition temperature ($T_g \approx 415$ °C) and two sharp exothermic crystallization peaks ($T_{cr1} = 490$ °C and $T_{cr2} = 510$ °C) are observed. Several other small peaks are observed at higher temperatures. The TGA curve also shows small weight gain by the sample at around 500 °C which is due to absorption of oxygen from the air. So DTA and TGA indicate the growth of crystalline phase by absorption of oxygen by the (4:3:3:4) sample at this temperature.

Chemical analysis by atomic absorption spectroscopy indicates the presence of 15.9 wt. % of copper atoms in

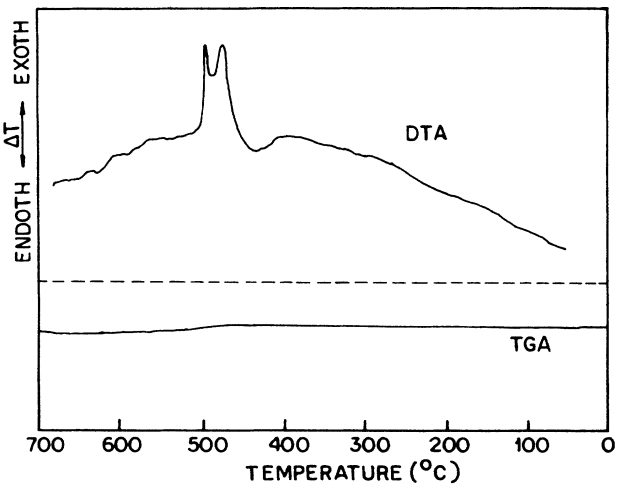

FIG. 2. DTA and TGA curves of the (4:3:3:4) glass.

the glass sample which agrees reasonably well with the theoretical value of 14.7%. The increase in copper ion concentration from that of the starting composition is due to loss of oxygen from the melt which is consequently responsible for the coexistence of different valency states of copper ion in the glass. Moreover, slight evaporation loss of Bi_2O_3 cannot be totally ruled out.

B. dc Conductivity

The logarithm of measured dc conductivity (σ_{dc}) of the (4:3:3:4) glass as a function of inverse temperature is shown in Fig. 3. The slope of the curve changes with temperature indicating temperature-dependent activation energy (W). This is a characteristic feature of hopping conduction as observed in many other transition-metal oxide glasses.[11,15,16,21,23] The activation energy of the glass decreases slowly below ≈ 300 K and at the lowest temperature of our investigation (80 K) it becomes 0.05 eV. This behavior is consistent with the polaron model of hopping conduction[13,14] which predicts an appreciable departure from a linear T^{-1} versus the $\ln\sigma_{dc}$ plot below a temperature $T_x \approx \Theta_D/2$ (Θ_D is the Debye temperature and is given by $k_B\Theta_D = h\nu_{ph}$, where k_B is Boltzmann's constant, h is Planck's constant, and ν_{ph} is the predominant phonon frequency). The value of this temperature (T_x) is better detected from the $\ln(\sigma_{dc}T)$ versus $1/T$ curve as discussed below. For all vanadate glasses Θ_D was calculated to be ≈ 600 K.[35] This is because of the fact that in different vanadate glasses the infrared spectra are nearly similar.[15,35] In the present copper oxide containing the (4:3:3:4) glass this type of hypothesis seems not to be strictly valid due to the higher density of vibrational modes appearing in the low-energy region of ir spectra.[36] For the (4:3:3:4) glass it is difficult to find average ω_{ph}, since the localized vibrational modes ascribed to the copper structural unit were not detected. A comparison with other transition-metal oxide glasses shows that the room-temperature (300 K) dc conductivity of the (4:3:3:4) glass is lower than those reported for the V_2O_5-P_2O_5,[15] V_2O_5-Bi_2O_3,[11] V_2O_5-TeO_2,[21] and Fe_2O_3-Bi_2O_3 (Ref. 19) glasses.

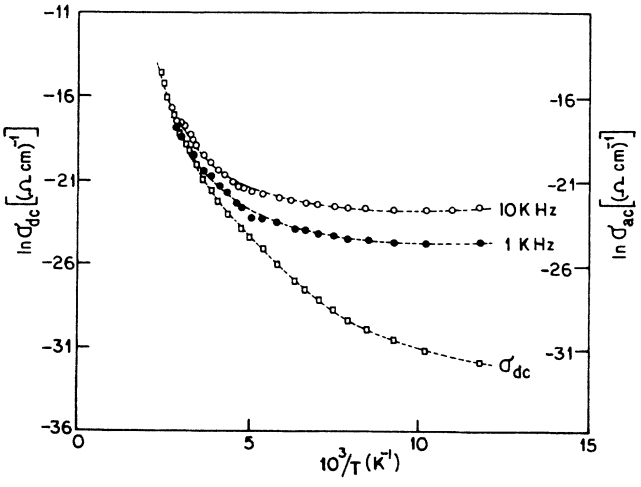

FIG. 3. $\ln\sigma$ (both σ_{dc} and σ_{ac}) vs T^{-1} curve for the (4:3:3:4) glass; (□), σ_{dc}, (●) σ_{ac} at $f=1$ kHz, and (○) σ_{ac} at $f=10$ kHz.

dc conductivity of the semiconducting TMO glasses is considered to be due to hopping of polarons (or electrons) between localized states and an expression for dc conductivity for the small-polaron hopping in the nonadiabatic approximation[13,14,37] is given by

$$\sigma_{dc} = \frac{\nu_{ph} N e^2 R^2}{k_B T} c(1-c)\exp(-2\alpha R)\exp(-W/k_B T) , \tag{1}$$

where N is the number of TMI sites per unit volume, e is the electronic charge, R is the average TMI site spacing, and c and α are, respectively, the ratio of the TMI concentration in the low valency state to the total TMI concentration and the wave-function decay constant such that $\exp(-2\alpha R)$ represents an electron overlap integral between nearest-neighbor sites. For many oxide glasses with different concentrations of TMI, the average TMI spacing (R) has a small distribution of values. A plot of $\ln\sigma_{dc}$ versus W at a fixed temperature for the P_2O_5-BaO-CuO (Ref. 23) and other TMO glasses[11,15,38] already affirmed that $\exp(-2\alpha R)$ is essentially constant for different concentration of the glass.

Assuming a strong electron-lattice interaction, the activation energy (W) in the high-temperature region ($T > \Theta_D/2$) where nearest-neighbor thermally activated hopping predominates results from polaron-hopping energy (W_H) and the disorder energy (W_D) which might exist between the initial and the final sites due to variation in the local environment of the ions. In the low-temperature region ($T < \Theta_D/4$) variable-range hopping (VRH) takes over from the thermally activated nearest-neighbor hopping and the activation energy is essentially due to disorder energy. Mott[13,14,37] have suggested an expression for activation energy (W) in the small-polaron model as,

$$W = W_H + \tfrac{1}{2}W_D \quad \text{for } T > \Theta_D/2 , \tag{2a}$$

$$W \simeq W_D \quad \text{for } T < \Theta_D/4 . \tag{2b}$$

The lowest temperature activation energy can be taken as a measure of disorder energy (W_D).

An estimate of the polaron radius (r_p) can be made from the relation,

$$r_p = \tfrac{1}{2}(\Pi/6N)^{1/3} , \tag{3}$$

where N is the total copper ion concentration. The calculated value of N for the (4:3:3:4) glass is shown in Table I. The polaron-hopping energy W_H can be calculated from the Austin and Mott's relation,[14]

$$W_H = \frac{e^2}{4\epsilon_p}(1/r_p - 1/R) , \tag{4}$$

where ϵ_p is the effective dielectric constant. The value of R ($\sim N^{1/3}$) is also given in Table I and should be con-

TABLE I. Different physical parameters for the (4:3:3:4) glass. W_H is calculated from Eq. (4). $\Delta W=[W(\text{at } 300\text{ K})-W_H]$.

Density ($g\,cm^{-3}$)	N ($ev^{-1}cm^{-3}$)	R (Å)	r_p (Å)	n	W (ev) 80 K	W (ev) 300 K	W_H (eV)	ΔW (eV)	ν_{ph} (Hz)	α ($Å^{-1}$)	T_g (°C)
5.93	8.53×10^{21}	4.89	1.97	2.5	0.05	0.30	0.18	0.12	1.18×10^{13}	0.67	415

sidered only as an estimated value. Since the r_p values are small, it suggests that the polaron is strongly localized. W_H can be calculated from Eq. (4) under the approximation of $\epsilon_p\simeq\epsilon_\infty\simeq n^2$ (n being the refractive index of the glass as shown in Table I). All the calculated parameters r_p, R, and W_H are shown in Table I. From the values of W and W_H the value of $W_D/2$ ($W-W_H=W_D/2$) is calculated to be 0.12 eV. A theoretical calculation of $W_D/2$ from Miller and Abrahams' theory,[39] however, gives $W_D/2=0.05$ eV which is lower than the corresponding calculated value (0.12 eV). Similar low values have also been reported for the vanadate glasses.[38,40] This discrepancy might be considered as the effect of the partial charge of the cations of the glass forming oxides (Bi_2O_3, CaO, etc.) on activation energy for hopping conduction in the TMO glasses.[38]

The presence of T^{-1} in the preexponential factor of the expression for σ_{dc} [Eq. (1)] suggests that a plot of $\ln(\sigma_{dc}T)$ versus $1/T$ would be more appropriate to distinguish between the high- and low-temperature region of dc conduction. In Fig. 4 we have plotted $\ln(\sigma_{dc}T)$ as a function of inverse temperature. It is observed from Fig. 4 that an appreciable deviation from linearity occurs at a temperature $T_x\simeq285$ K. According to the small-polaron model of hopping conduction[13,14] this should happen at a temperature $T_x=\Theta_D/2$. Thus one has an estimate of Debye temperature ($\Theta_D\simeq570$ K) for the (4:3:3:4) glass. The phonon frequency (ν_{ph}) is calculated to be $\simeq1.18\times10^{13}$ Hz (using the relation $k_B\Theta_D=h\nu_{ph}$).

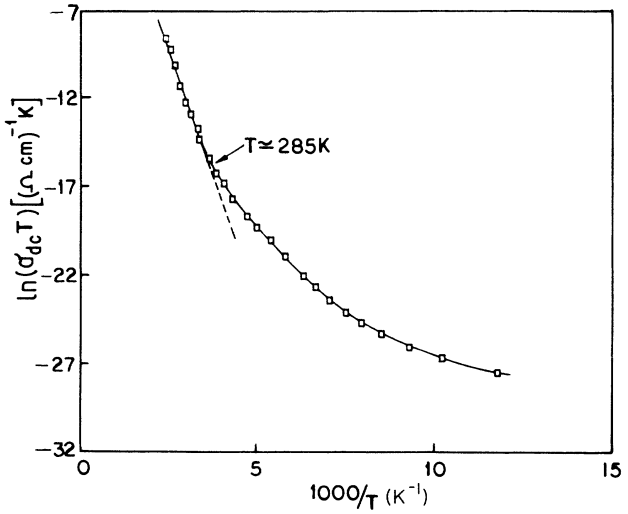

FIG. 4. $\ln(\sigma_{dc}T)$ vs T^{-1} curve for the (4:3:3:4) glass.

The small-polaron coupling constant (γ) which is a measure of the electron-phonon interaction in the (4:3:3:4) glass might also be estimated from the simple relation,[14]

$$\gamma=W_P/\hbar\omega_{ph}\ , \tag{5}$$

where W_P is the polaron binding energy and is approximately given by $W_P\approx2W_H$, $\hbar=h/2\Pi$, and $\omega_{ph}=2\Pi\nu_{ph}$. Using the values of W_H and ν_{ph} from Table I one gets $\gamma\approx7.4$. Austin and Mott[14] have suggested that a value of $\gamma>4$ usually indicates strong electron-phonon interaction in the solid. This value of γ can be further used to evaluate the effective mass of the polaron. The effective polaron mass (m_p) in the adiabatic approximation [the reason for considering the hopping process in the (4:3:3:4) glass in the adiabatic approximation will be discussed later in this section] is given by[14,37]

$$m_p=(\hbar/2\omega_{ph}R^2)\exp(\gamma)\ . \tag{6}$$

Using $\gamma=7.4$, and the values of R and ν_{ph} from Table I, one finds $m_p/m_e\simeq5.35\times10^3$ (m_e is the electron rest mass) which seems to be quite large. However, higher values of $\gamma(\approx14)$ and hence very large values of m_p ($\approx10^7m_e$) in the vanadium phosphate glass have been reported[35] earlier.

A check of the nature of hopping can, in principle, be made using Holstein's condition.[41] The polaron bandwidth J should satisfy the following relation:

$$J>(2k_BTW_H/\Pi)^{1/4}(\hbar\omega_{ph}/\Pi)^{1/2}$$

for adiabatic hopping ,

$$J<(2k_BTW_H/\Pi)^{1/4}(\hbar\omega_{ph}/\Pi)^{1/2} \tag{7}$$

for nonadiabatic hopping .

The condition for the small-polaron formation is $J\le W_H/3$. An estimate of J can be made by the approximate relation.

$$J\sim e^3[N(E_F)]^{1/2}/\epsilon_p^{3/2}\ , \tag{8}$$

where $N(E_F)$ is the density of state at the Fermi level. An estimate of $N(E_F)$ was obtained from Mott's $T^{-1/4}$ analysis (discussed later) of the low-temperature conductivity data of the (4:3:3:4) glass. The estimated value of $N(E_F)$ is of the order of 10^{21} $eV^{-1}cm^{-3}$. ϵ_p is calculated from the relation $\epsilon_p\simeq n^2$ (the value of n is shown in Table I). Equation (8) gives $J\sim0.11$ eV with these values of $N(E_F)$ and ϵ_p. The value of the right-hand side of Eq. (7) (with W_H and ν_{ph} from Table I) is $\simeq0.028$ eV. There-

fore, the condition for adiabatic hopping appears to be satisfied for the (4:3:3:4) glass. This also suggests that the tunneling term $\exp(-2\alpha R)$ in Eq. (1) may not be dominant as has been suggested by Sayer and Mansingh[15] for transition-metal phosphate glasses.

Schnakenberg[42] suggested that with the lowering of temperature the multiphonon processes are replaced by a single-phonon (optical-phonon) process and at the lowest temperatures the polaron hops with one or more acoustic phonons making up differences between sites. The ratio of high- and low-temperature activation energies (W and W', respectively) is expressed as,

$$\frac{W}{W'}=\frac{\tanh(\hbar\omega_{\rm ph}\beta/4)}{\hbar\omega_{\rm ph}\beta/4}\ , \tag{9}$$

where $\beta=1/k_BT$. In Fig. 5 the experimental as well as the theoretical values of W/W' given by Eq. (9) are plotted against $1/T$ for the (4:3:3:4) glass. From this figure one finds that the experimental values of the activation energy decrease with increasing temperature but that the quantitative fit of the experimental values with the theoretical curve is rather poor. This indicates that the increase in the magnitude of conductivity with temperature cannot be attributed to the decrease in activation energy alone.

At low temperature where the polaron binding energy is small and the static disorder energy of the glass plays a dominant role in the conduction process, Mott's $T^{-1/4}$ analysis for the variable-range hopping can also be made. So we have plotted $T^{-1/4}$ versus $\ln\sigma_{\rm dc}$ (Fig. 6) to check the applicability of Mott's formula[13,37] in the present (4:3:3:4) glass. According to Mott's formula the conductivity for the variable-range hopping at low temperatures is given by

$$\sigma_{\rm dc}=A\exp(-B/T^{1/4}) \tag{10}$$

where

$$A=e^2N(E_F)R^2\ .$$

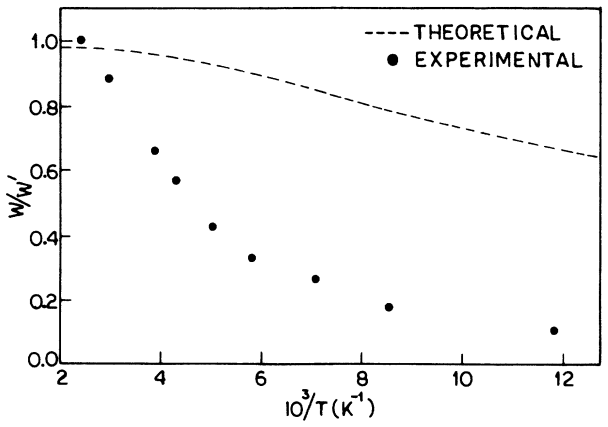

FIG. 5. Plot of W/W' vs $10^3/T$ for the (4:3:3:4) glass; (— — —) theoretical curves and (●) experimental points.

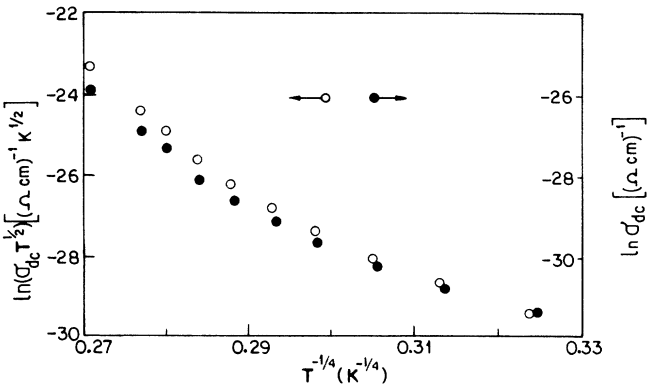

FIG. 6. Plot of (a) $\ln\sigma_{\rm dc}$ vs $T^{-1/4}$ (●), and (b) $\ln(\sigma_{\rm dc}T^{1/2})$ vs $T^{-1/4}$ (○) for the (4:3:3:4) glass.

The slope of the $T^{-1/4}$ versus in $\sigma_{\rm dc}$ curve gives the parameter B, where,

$$B=2.1[\alpha^3/k_BN(E_F)]^{1/4}\ . \tag{11}$$

Equation (10) suggests that the $T^{-1/4}$ versus $\ln\sigma_{\rm dc}$ plot should be linear. The same plot for the (4:3:3:4) glass (Fig. 6), however, indicates the presence of two linear regions above and below $T\approx108$ K with two different slopes. From the slope of the curve below 108 K and using the value of α [obtained from the fitting of experimental data with Eq. (1) and shown in Table I] the value of $N(E_F)$ is calculated to be $\approx10^{21}$ eV^{-1}cm^{-3} which is comparatively higher than the value obtained from ac conductivity data (Table II, discussed below). The disorder energy (W_D) can also be estimated from the slope of Fig. 6 by

$$B=2.4[W_D(\alpha R)^3/k_B]^{1/4}\ . \tag{12}$$

The calculated value of W_D, using the value of α and R from Table I, is found to be ≈1.5 eV. This value of W_D is much higher than the low-temperature activation energy (≈0.05 eV) obtained theoretically.[39] This type of high value of W_D was also reported by Dhawan *et al.*[21] for the V_2O_5-TeO_2 glasses.

In an alternative way Greaves[43] suggested a variable-range hopping conduction in the intermediate temperature range and derived the expression,

$$\sigma_{\rm dc}T^{1/2}=C\exp(-B/T^{1/4})\ , \tag{13}$$

where B and C are constants, B is given by the same expression as given by Eq. (11). The plot of $\ln(\sigma_{\rm dc}T^{1/2})$ versus $T^{-1/4}$ is shown in Fig. 6 for the (4:3:3:4) glass. The straight line nature of this curve, as suggested by the Greaves' relation [Eq. (13)], is observed only over a small range of temperature but the general behavior of the curve appears to deviate from linearity with the increase of temperature.

Considering the hopping within energy k_BT of the Fermi level Austin and Mott[14] obtained the expression for ac

TABLE II. Different parameters obtained from ac conductivity and dielectric constant data. The values of W_{HO} and α are obtained from the OLPT model using $\ln(\omega\tau_0)=-18.8$.

τ_0 (sec)	ϵ (1 kHz)	R_ω (Å)	N ($ev^{-1}cm^{-3}$)	s 80 K	s 400 K	W_{HO} (eV)	α ($Å^{-1}$)
10^{12}	18	7.7	1.39×10^{19}	0.87	0.22	0.29	0.61

conductivity (σ_{ac}) as

$$\sigma_{ac}=\tfrac{1}{3}\Pi e^2k_BTN(E_F)^2\alpha^{-5}[\ln(\nu_{ph}/\omega)]^4 . \quad (14)$$

Substituting the values of ν_{ph} and α (from Table I) we find $N(E_F)\approx1.17\times10^{20}$ $eV^{-1}cm^{-3}$ for 1 kHz and $N(E_F)\approx4.17\times10^{19}$ $eV^{-1}cm^{-3}$ for 10 kHz from the experimental values of $\sigma_{ac}(\omega)$ at low temperature (discussed below). These values of $N(E_F)$ for the (4:3:3:4) glass are close to the values obtained from the correlated barrier hopping (CBH) model of ac conductivity[31–33] as discussed in the next section.

C. ac conductivity and dielectric constant

The ac conductivity $\sigma_{ac}(\omega)$ and dielectric constant (ϵ') of the (4:3:3:4) glass have been measured between 80–420 K for two different frequencies (1 and 10 kHz). The ac conductivity $\sigma_{ac}(\omega)$ as a function of temperature is shown in Fig. 3. It is observed from this figure that, in common with many other amorphous semiconductors, the temperature dependence of $\sigma_{ac}(\omega)$ is much less than σ_{dc} at low temperatures and is not activated in behavior. However, the temperature and its frequency dependences become strong with the increase of temperature. Ultimately the measured conductivities at all frequencies coincide with σ_{dc} at higher temperatures.

The ac conductivity as shown in Fig. 3 was calculated by subtracting the measured dc conductivity from the measured total frequency-dependent conductivity $\sigma_t(\omega)$ such that

$$\sigma_{ac}(\omega)=\sigma_t(\omega)-\sigma_{dc} . \quad (15)$$

When ac and dc conductivities are due to the same process and σ_{dc} is simply $\sigma_{ac}(\omega)$ (in the limit $\omega\rightarrow0$), the separation given in Eq. (15) is no longer useful.

Like many amorphous semiconductors and insulators, the ac conductivity of the (4:3:3:4) glass was found to follow the equation

$$\sigma_{ac}(\omega)=A\omega^s , \quad (16)$$

where A is a constant dependent on temperature and s is the frequency exponent, generally less than unity. All that is required to give this behavior is that the loss mechanism should have a very wide range of possible relaxation times.

The estimated frequency exponent s is shown in Fig. 7 as a function of temperature. The variation of the exponent s at room temperature with different frequencies is shown in Fig. 8. It is interesting to mention that such a sharp frequency dependence of s has not been observed for the vanadate or similar other oxide glasses.[11,18,19]

Many different theoretical explanations[31,32] for the ac conduction in amorphous semiconductors have been proposed to account for the frequency and temperature dependence of σ_{ac} and s. It is commonly believed that the pair approximation holds, namely, the dielectric loss occurs because the carrier motion is considered to be localized within a pair of sites. In essence, two distinct processes have been proposed for the relaxation mechanism, namely, quantum-mechanical tunneling through the barrier separating two equilibrium positions and classical hopping of a carrier over the barrier or some combination or variant of the two, and it is variously assumed that the electrons (or polarons) or atoms are the carriers responsible for the conduction. In what follows, the ac conductivity data for the (4:3:3:4) glassy semiconductor are analyzed in the light of the existing theoretical models.

1. *Quantum-mechanical tunneling (QMT) model*

Several authors[14,30,32,44] calculated with the pair approximation, the ac conductivity data for single-electron motion undergoing QMT, and obtained the expression for the ac conductivity as

$$\sigma_{ac}(\omega)=Ce^2k_BT\alpha^{-1}[N(E_F)]^2\omega R_\omega^4 , \quad (17)$$

where C is a numerical constant which slightly varies according to different authors, but may be taken as $\Pi^4/24$ (Refs. 32 and 44], and R_ω is the hopping distance at frequency ω, given by

$$R_\omega=(2\alpha)^{-1}\ln(1/\omega\tau_0) , \quad (18)$$

where τ_0 is a characteristic relaxation time. The frequen-

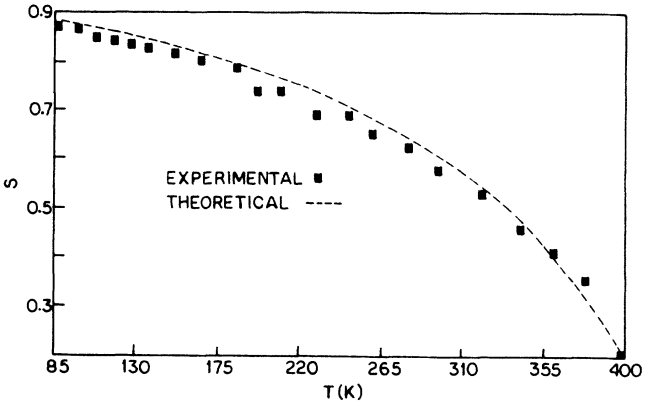

FIG. 7. Temperature variation of s of the (4:3:3:4) glass at 1 kHz; (■) experimental points, and (— — —) theoretical curve obeying Eq. (27).

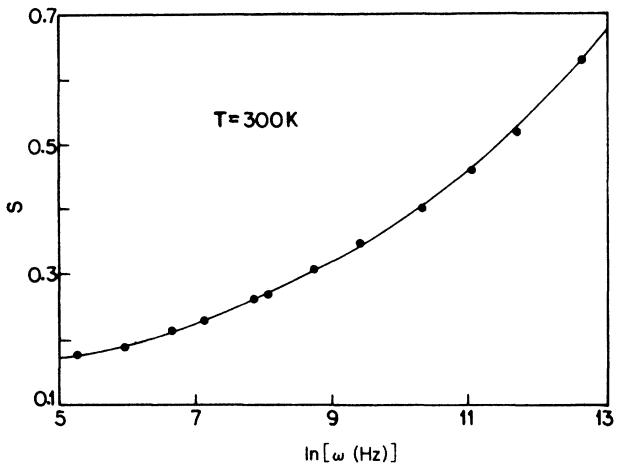

FIG. 8. Variation of s with frequency at room temperature (300 K).

cy exponent s in this model is obtained from

$$s=1-4/[\ln(\omega\tau_0)] \ . \tag{19}$$

Therefore, for the QMT model, $\sigma_{ac}(\omega)$ is linearly dependent on temperature T [Eq. (17)], but the exponent s is temperature independent and frequency dependent [Eq. (19)]. For typical values of the parameters $\tau_0=10^{-13}$ sec and $\omega/2\Pi=10^4$ Hz, a value of $s=0.81$ is obtained from Eq. (19). However, it is clearly observed for the (4:3:3:4) glass that the exponent s decreases with increase of temperature (Fig. 7) and increases with increase of frequency at a fixed temperature (Fig. 8). Furthermore, the QMT model predicts a linear temperature dependence of $\sigma_{ac}(\omega)$. But our experimental results, as shown in Fig. 9, indicate a much sharper increase of $\sigma_{ac}(\omega)$ with the rise of temperature particularly in the high-temperature regime. A temperature-dependent frequency exponent can

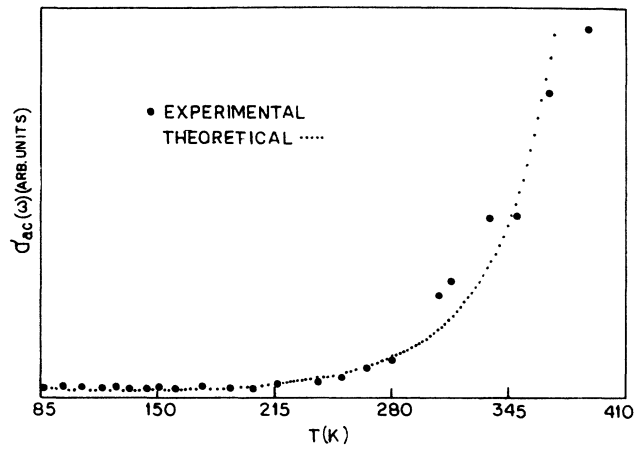

FIG. 9. Thermal variation of $\sigma_{ac}(\omega)$ at 1 kHz; (●) experimental, and (—·—·—·) theoretical curve obeying the CBH model.

be obtained within the framework of the QMT model by assuming that the carriers form nonoverlapping small polarons. In our case, however, the frequency exponent decreases with increase in temperature (Fig. 9). The simple QMT model also predicts that s should decrease with increase of frequency [Eq. (19)]. But in the (4:3:3:4) glassy semiconductor s increases sharply in the range of our investigation, viz. (10^2–10^5 Hz). Thus for the above reasons the QMT model clearly fails to explain the experimental ac conductivity data of the (4:3:3:4) glass.

2. *Overlapping-large-polaron tunneling (OLPT) model*

In this case, as suggested by Long,[32] the large-polaron wells of the two sites overlap and thereby reduces the polaron-hopping energy. In this case one has

$$W_H=W_{HO}(1-r_p/R) \ , \tag{20}$$

where W_{HO} is defined as

$$W_{HO}=e^2/4\epsilon_p r_p \ . \tag{20a}$$

Assuming R as a random variable, $\sigma_{ac}(\omega)$ in this model[32] comes out to be of the form

$$\sigma_{ac}(\omega)=\frac{\Pi^4}{12}e^2(k_BT)^2[N(E_F)]^2\bar{\chi} \ , \tag{21}$$

where

$$\bar{\chi}=\omega R_\omega^2/(2\alpha k_BT+W_{HO}r_p/R_\omega^2) \ .$$

The hopping length R_ω is determined from the quadratic equation

$$(R'_\omega)^2+[\beta W_{HO}+\ln(\omega\tau_0)]R'_\omega-\beta W_{HO}r'_P=0 \ . \tag{22}$$

Here $R'_\omega=2\alpha R_\omega$, $r'_p=2\alpha r_p$, and $\beta=1/k_BT$. The exponent s in the OLPT model can be evaluated from

$$1-s=\frac{8\alpha R_\omega+6\beta W_{HO}r_p/R_\omega}{(2\alpha R_\omega+\beta W_{HO}r_p/R_\omega)^2} \ . \tag{23}$$

Thus the OLPT model predicts that s should be both temperature and frequency dependent [cf. Eq. (23)] and that the frequency exponent s decreases from unity with the increase of temperature. For large values of r'_p's the values of s continue to decrease with increasing temperature, eventually tending to the value of s predicted by the simple QMT model, where for small values of r'_p's the exponent s exhibits a minimum at a certain temperature and subsequently increases in a similar fashion as in the case of small-polaron QMT. Thus, it appears that the OLPT model should better fit the experimental ac conductivity data of the (4:3:3:4) glass, since the experimental values of s decrease with the increase of temperature (Fig. 7). To verify this, the frequency exponent s is plotted in Fig. 10 as a function of k_BT/W_{HO} similar to our earlier paper on the semiconducting oxide glasses.[19,22] The value of W_{HO} (Table II) was calculated from Eq. (20a) using the values of r_p and ϵ_p from dc conductivity data (shown in Table I). The theoretical curves given by Eq. (23) are also drawn in Fig. 10 for various values of r'_p.

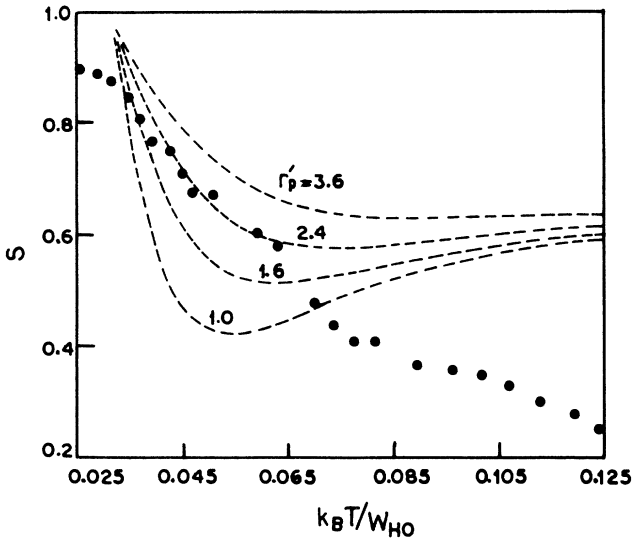

FIG. 10. Plot of k_BT/W_{HO} vs s: ●, experimental points; — — —, theoretical curves.

The best fit to the experimental data (in the low-temperature region, for $k_BT/W_{HO}<0.6$) has been observed for the value of $r'_p=2.4$ as shown in Fig. 10. The decay constant α can be estimated from the relation $r'_p=2\alpha r_p$ using this value of r'_p. The estimated value of α as shown in Table II agrees fairly well with the value obtained from the dc conductivity data shown in Table I. However, the values of r_p, being smaller than R, appear to be inconsistent with the basic premise of the OLPT model (for the large-polaron case). At higher temperatures, the experimental data for s neither lie between the theoretical curves (Fig. 10), nor are they minimum according to the requirement of the OLPT model. This is also true for the V_2O_5-Bi_2O_3 (Ref. 22) and Fe_2O_3-Bi_2O_3 (Ref. 19) glasses.

The OLPT model also predicts [cf. Eq. (21)] an appreciably stronger temperature dependence of $\sigma_{ac}(\omega)$ in the temperature regime where the frequency exponent s is a decreasing function of temperature. The functional form of the temperature dependence of $\sigma_{ac}(\omega)$ shown by Eq. (21) is a complicated one and cannot be expressed simply as T^v (with v constant over a wide range of temperature). Nevertheless, at low temperatures ($k_BT/W_{HO}<0.04$–0.05) the hopping length R has an approximately constant temperature dependence, $R\sim T^{1.25}$ (for $r'_p\approx 2.5$) and insertion of this value in Eq. (21) yields $\sigma_{ac}(\omega)\sim T^6$ for the uncorrelated case. This is obviously at variance with the much weaker temperature dependence exhibited by the low-temperature data of the present work (Fig. 9) and even if the correlated form[31] of the OLPT model is invoked, the said dependence is predicted to decrease only to $\sigma_{ac}(\omega)\sim T^4$. It, therefore, appears that the temperature dependence of the ac conductivity is not really met within the framework of the OLPT model developed by Long.[32]

3. *Correlated-barrier-hopping (CBH) model*

Another model for ac conductivity which correlates the relaxation variable W with the intersite separation R was proposed by Pike[33] for single-electron hopping and extended by Elliott[31] for the two electrons hopping simultaneously. For the neighboring sites at a separation R, the Coulomb wells overlap, resulting in a lowering of the effective barrier height from W_M to a value W, which for the case of two electrons hopping is given by[31,32]

$$W=W_M-2e^2/\Pi\epsilon\epsilon_0 R \ , \tag{24}$$

where ϵ and ϵ_0 are, respectively, the dielectric constant of the material and the permittivity of the free space. The ac conductivity in this CBH model, in the narrow-band limit, is given by[33]

$$\sigma_{ac}(\omega)=\frac{1}{24}\Pi^3N^2\epsilon_0\epsilon\omega R_\omega^6 \ . \tag{25}$$

The hopping distance R_ω is given by

$$R_\omega=(2e^2/\Pi\epsilon\epsilon_0)[W_M+k_BT\ln(1/\omega\tau_0)] \ . \tag{26}$$

The frequency exponent s with the CBH model is given by

$$1-s=\frac{6k_BT}{W_M-k_BT\ln(1/\omega\tau_0)} \ . \tag{27}$$

Therefore, according to the CBH model, a temperature-dependent frequency exponent s is predicted, with s increasing towards unity as $T\rightarrow 0$, which is in marked contrast with the QMT or simple hopping over the barrier model,[33] and therefore, it might be a possible contending model for the explanation of the ac conductivity of the (4:3:3:4) glass in its semiconducting phase.

A critical test of the CBH model comes from the temperature dependence of the ac conductivity and its frequency exponent. Our experimental results, as shown in Figs. 7 and 9, exactly show similar nature as suggested by the CBH model. In Fig. 7 the experimental values of s are shown as a function of temperature along with the theoretical curve obeying Eq. (27) (with $\omega/2\Pi=1000$ Hz and $W_M=0.88$ eV). Here W_M is taken as twice the high-temperature activation energy obtained from our dc conductivity results as reported in Sec. III B and in Table I. The best fit with the experimental curve is obtained with $\tau_0=10^{-12}$ sec which seems to be quite reasonable and nearly equal to the values obtained for other semiconducting oxide glasses.[32,38] The little discrepancy existing between the theoretical and the experimental values as indicated by Fig. 7 might be due to some inaccuracy in the determination of the barrier height (W_M). At this point it would be worthwhile to mention that the correlation between the barrier height and hopping distance might cause appreciable deviation of $\sigma_{ac}(\omega)$ as well as of s from the corresponding theoretical values. Using the same value of $W_M(=0.88$ eV) and $\tau_0(=10^{-12}$ sec) we have calculated the value of R_ω from Eq. (22) which was found to be $\approx 7.7\times 10^{-8}$ cm. Putting this value of R_ω and ϵ from our experimental dielectric constant data in Eq. (25), N was calculated to be $\approx 1.39\times 10^{19}$ eV^{-1} cm^{-3}.

The estimated value of N (Table II) seems to be rather low which may be due to the fact, as suggested by Linsley *et al.*,[45] that some of the sites may remain inactive due to the glass structure resulting in a lower number of sites actually participating in the conduction process.

The temperature dependence of $\sigma_{ac}(\omega)$ in the CBH model is given by

$$\sigma_{ac}(\omega) \propto T^{\nu} , \tag{28}$$

where

$$\nu = (1-s)\ln(1/\omega\tau_0) .$$

In Fig. 9 we have plotted the experimental temperature variation of $\sigma_{ac}(\omega)$ along with the theoretical temperature dependence obeying Eq. (28). A reasonably good fit of the experimental values with the theoretical curve indicates the applicability of the CBH model in explaining the experimental ac conductivity data of the (4:3:3:4) glass.

D. Dielectric constant

The dielectric constant (ϵ') and the loss tangent tanδ were also measured simultaneously along with the ac conductivity measurement using the capacitance bridge technique as discussed earlier.

The temperature variation of ϵ' and tanδ for two fixed frequencies 1 and 10 kHz are shown in Fig. 11. Both ϵ' and tanδ are found to increase with the increase of temperature. The curve corresponding to 10 kHz (Fig. 11) shows a peak at about 366 K in the ϵ' versus T curve which is a common feature indicating the Debye-type dielectric relaxation process[46,47] characterized by a relaxation frequency f_0 (where $f_0 = 1/2\Pi\tau_0$, τ_0 being the dielectric relaxation time). The loss peak occurs at a temperature at which the measuring frequency equals the relaxation frequency. For this (4:3:3:4) glass the loss curve corresponding to 1 kHz shows no such peak within the range of our investigation. In Fig. 12 we have plotted ϵ'

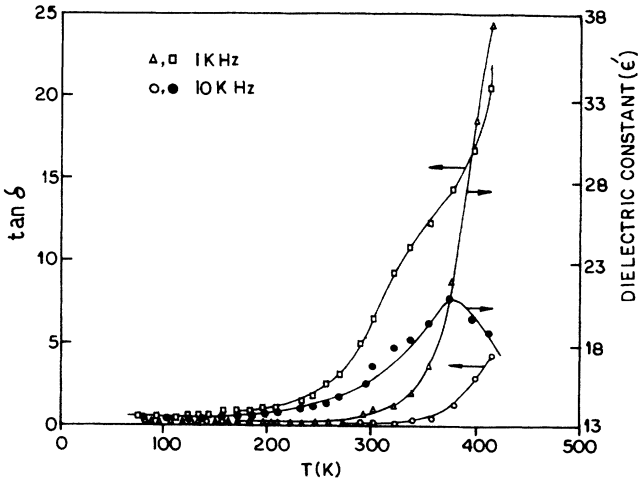

FIG. 11. Temperature variation of ϵ' and tanδ for the (4:3:3:4) glass at two fixed frequencies.

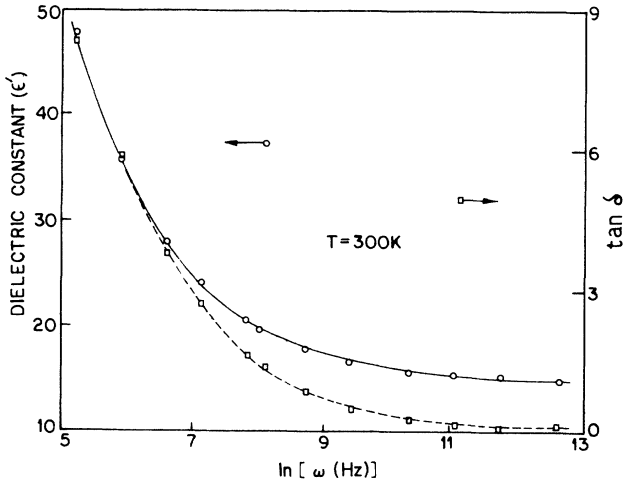

FIG. 12. Frequency variation of (a) ϵ' (○) and (b), tanδ (□) of the (4:3:3:4) glass at 300 K.

versus $\ln(\omega)$ as well as tanδ versus $\ln(\omega)$ at room temperature (300 K). Both ϵ' and tanδ are found to decrease with increase of frequency which is consistent with the behavior of ac conductivity discussed in Sec. III C.

E. Imaginary part of ac conductivity

Real [denoted by $\sigma_1(\omega)$] and the imaginary part [denoted by $\sigma_2(\omega)$] of the ac conductivity are related via Kramers-Kronig relation. The values of $\sigma_1(\omega)$ and $\sigma_2(\omega)$ are also related to the dielectric constant. The total measured capacitance $C_{tot}(\omega)$, like conductance, can also be expressed into two parts, arising from different processes, viz.,

$$C_{tot}(\omega) = C(\omega) + C_{\infty} , \tag{29}$$

where the dispersive term $C(\omega)$ is determined by the loss measurements and the nondispersive term C_{∞} is determined by the high-frequency atomic and dipolar vibrational transitions. Several methods[32] for determining $C(\omega)$ from the capacitance data have been proposed. In the present work, $C(\omega)$ was estimated from the numerical differentiation of the capacitance whereupon the constant term involving C_{∞} drops out. The ratio of the imaginary to the real part of the conductivity is then calculated from the relation,

$$\lambda = \sigma_2(\omega)/\sigma_1(\omega) = \omega C(\omega)/G(\omega) , \tag{30}$$

where $G(\omega)$ is the conductance at frequency ω. It has been shown[32] that λ have characteristically different forms for the various mechanisms of dielectric relaxation. Thus from the QMT model one finds

$$\lambda = -(2/5\Pi)\ln(\omega\tau_0) \tag{31}$$

and the CBH model, on the otherhand, gives to a first approximation for small $k_B T/W_M$,

$$\lambda = -(2/\Pi)\ln(\omega\tau_0)[1 + (3k_B T/W_M)\ln(\omega\tau_0)] . \tag{32}$$

It might be noted that the CBH model predicts a temperature dependence of λ, whereas the QMT model does not. For the OLPT model λ behaves similar to the behavior of that exhibited by the QMT model at high temperatures and at low temperatures the behavior is similar to that exhibited by the CBH model.

Calculation of the ration λ using our experimental data indicates that λ is temperature dependent which implies inapplicability of the QMT model for the (4:3:3:4) glass. However, for the CBH model [Eq. (32)] the fit between theory and experiment is found to be reasonably good which supports the applicability of the CBH model for the ac conductivity data of the (4:3:3:4) glassy semiconductor as discussed in Sec. III C. However, it should be noted that Eq. (32) for the CBH model is also an approximate one; higher-order terms become important at higher temperatures.

IV. CONCLUSION

From our experimental observation of electrical properties it appears that the electrical conduction in the $Bi_4Sr_3Ca_3Cu_4O_x$ glass containing the transition metal copper ions, a polaron model is generally applicable. There is some evidence that the hopping of polarons occurs in the adiabatic regime similar to many vanadate glasses.[11,15,35] However, a conclusive decision as to whether the polaron is actually in the adiabatic regime requires an independent estimate of polaron bandwidth J from other experimental observations. Measurement of Hall mobility might be useful in finally resolving the controversy. Furthermore, investigations with glasses containing different concentrations of the transition metal (Cu for the present Bi-Sr-Ca-Cu-O glass) would be very helpful to enlighten the matter. However, it should be noted here that for other concentrations of TMI the glasses could not be made superconducting above 77 K by annealing the glasses. Since the (4:3:3:4) glass becomes superconducting by annealing we have concentrated our attention on the characterization of this glass first.

The general feature of the temperature-dependent dc conductivity of the (4:3:3:4) oxide glass were similar to that of the other semiconducting oxide glasses like V_2O_5-P_2O_5, V_2O_5-Bi_2O_3, etc. In the high temperature (above $\approx$285 K) the conduction process is dominated by thermally activated nearest-neighbor hopping of small polaron. In the intermediate and low-temperature region the VRH conduction appears to be more appropriate. The fitting of the experimental conductivity data with Greaves'[43] and Mott's[13] relation for VRH at intermediate and low temperature shows reasonably good qualitative agreement although the quantitative fit appears not to be very good. Moreover, the magnitudes of some of the model parameters obtained for the (4:3:3:4) oxide glass (Tables I and II) (viz., r_p, r_p', α, and W_{HO}) are found to differ appreciably from those of the other oxide glasses mentioned above. The temperature and frequency dependences of ac conductivity and the dielectric constant were considered to be related to the Debye-type relaxation process. The CBH model, when fitted with the experimental ac conductivity data yielded reasonable values of the barrier height and relaxation time agreeing with those obtained from the dc conductivity data. The QMT model is consistent with the temperature dependence of the ac conductivity at low temperature. However, this model completely fails to predict the temperature dependence of the frequency exponent, even at low temperature. Similarly, the overlapping large-polaron tunneling model predicts the temperature dependence of the ac conductivity much higher than that shown by the experimental data, although the temperature dependence of the frequency exponent is in agreement with this model in the low-temperature region.

Finally, since this (4:3:3:4) glass becomes superconducting with $T_c \approx 80$ K, when properly annealed, the results of the present investigations might help for an in-depth understanding of the mechanism of high-temperature superconductivity in oxides like Bi-Sr-Ca-Cu-O, Y-Ba-Cu-O, etc. systems of current interest. It is now well known[48–50] that the concept of polarons and bipolaron formalism are being invoked in many recent theories of high-temperature superconductivity in oxides.

ACKNOWLEDGMENTS

The authors are grateful to Professor S. P. Sengupta, Professor N. Ray Choudhury, Dr. A. K. Ghoshal, and Mr. G. Basak for their help and cooperation while doing some structural and DTA studies of our samples.

[1]T. Yoshida, H. Hirashima, and M. Kato, Yogyo-Koykai-Shi (in Japanese) **93**, 244 (1985).
[2]H. Hirashima, Y. Watanabe, and T. Yoshida, J. Non-Cryst. Solids **95/96**, 825 (1987).
[3]J. D. Mackenzie, *Modern Aspects of Vitreous State* (Butterworth, Washington, 1964), Vol. 3, p. 126.
[4]A. Ghosh and B. K. Chaudhuri (unpublished).
[5]Y. Sakuri and J. Yamaki, J. Electrochem. Soc. **132**, 512 (1985).
[6]S. Nakamura and N. Ichinose, J. Non-Cryst. Solid **95/96**, 847 (1987).
[7]K. K. Som and B. K. Chaudhuri (unpublished).
[8]B. K. Chaudhuri, K. K. Som, and S. P. Sengupta, J. Mater. Sci. Lett. **8**, 520 (1989).
[9]K. K. Som, A. K. Ghoshal, and B. K. Chaudhuri, J. Mater. Sci. Lett. **8**, 749 (1989).
[10]T. Komatsu, K. Imai, R. Sato, K. Matusita, and T. Yamashita, Jpn. J. Appl. Phys. Pt. 2 **27**, L533 (1988); **27**, L550 (1988). V. Skumryev, R. Puzniak, N. Kappe, Han Zheng-he, M. Pont, H. Medelins, D. X. Chen, and K. V. Rao, Physics B + C (Amsterdam) **152C**, 315 (1988).
[11]A. Ghosh and B. K. Chaudhuri, J. Non-Cryst. Solids **83**, 151 (1986).
[12]A. Ghosh and B. K. Chaudhuri, *Metallic and Semiconducting Glasses-II,* edited by A. K. Bhatnagar (Trans Tech, Aedermannsdorf, Switzerland, 1986), pp. 515–518.
[13]N. F. Mott, J. Non-Cryst. Solid **1**, 1 (1968).
[14]I. G. Austin and N. F. Mott, Adv. Phys. **18**, 41 (1969).
[15]M. Sayer and A. Mansingh, Phys. Rev. B **6**, 4629 (1972).
[16]A. P. Schmid, J. Appl. Phys. **39**, 3140 (1968).
[17]L. Murawski, C. H. Chung, and J. D. Mackenzie, J. Non-

Cryst. Solids **32**, 91 (1979).
[18]A. Ghosh and B. K. Chaudhuri, J. Mater. Sci. **22**, 2369 (1987). L. Murawski, Philos. Mag. B **50**, L69 (1984).
[19]B. K. Chaudhuri, K. Chaudhuri, and K. K. Som, J. Phys. Chem. Solids (to be published).
[20]A. Mansingh, R. P. Tandon, and J. K. Vaid, Phys. Rev. B **21**, 4829 (1980).
[21]A. Mansingh, J. K. Vaid, and R. P. Tandon, J. Phys. C **8**, 1023 (1975). V. K. Dhawan and A. Mansingh, J. Non-Cryst, Solids **51**, 87 (1982).
[22]B. K. Chaudhuri, K. Chaudhuri, and K. K. Som (unpublished).
[23]A. Duran, J. R. Jurado, and J. M. F. Navarro, J. Non-Cryst. Solids, **79**, 333 (1986).
[24]J. G. Bednorz and K. A. Muller, Z. Phys. B **64**, 189 (1986).
[25]H. Maeda, Y. Tanaka, and M. Fukutomi, Jpn. J. Appl. Phys. Lett. **27**, L209 (1988).
[26]Z. Z. Sheng and A. M. Hermann, Nature, **332**, 138 (1988).
[27]J. M. Tarascon, Y. Le Page, L. H. Greene, B. G. Bagley, P. Barboux, D. M. Hwang, G. W. Hull, W. R. McKinnon, and M. Giroud, Phys. Rev. B **38**, 2504 (1988).
[28]R. J. Cava, R. B. Van Dover, B. Battlog, and E. A. Reitman, Phys. Rev. Lett. **58**, 408 (1987).
[29]D. J. Scalapino, D. R. Clarke, J. Clarke, R. E. Schwall, A. E. Clark, and D. K. Finnemore, Cryogenics **28**, 711 (1988).
[30]M. Pollak and T. H. Geballe, Phys. Rev. **122**, 1742 (1961).
[31]S. R. Elliot, Philos. Mag. **36**, 1291 (1977). Adv. Phys. **36**, 135 (1987).
[32]A. R. Long, Adv. Phys. **31**, 553 (1982).
[33]G. E. Pike, Phys. Rev. B **6**, 1572 (1972).
[34]C. H. Chung and J. D. Mackenzie, J. Non-Cryst. Solids **42**, 357 (1980).
[35]M. Sayer, A. Mansingh, J. M. Reyes, and G. Rosenblatt, J. Appl. Phys. **42**, 2857 (1971).
[36]B. K. Chaudhuri and K. K. Som (unpublished).
[37]N. F. Mott and E. A. Davis, *Electronic Processes in Non-Crystalline Materials*, 2nd ed. (Clarendon Oxford, 1979).
[38]C. H. Chung, J. D. Mackenzie, and L. Murawski, Rev. Chim. Miner. **16**, 308 (1979).
[39]A. Miller and E. Abrahams, Phys. Rev. **120**, 745 (1960).
[40]J. Appel, *Solid State Physics*, edited by F. Seitz, D. Turnbull, and H. Ehrenreich (Academic, New York, 1968), p. 193, Vol. 21.
[41]T. Holstein, Ann. Phys. (N.Y.) **8**, 343 (1959).
[42]J. Schnakenberg, Phys. Status Solidi **28**, 623 (1968).
[43]G. N. Greaves, J. Non-Cryst, Solids **11**, 427 (1973).
[44]A. L. Efros, Philos. Mag. B **43**, 829 (1981).
[45]G. S. Linsley, A. E. Owen, and F. M. Hayatte, J. Non-Cryst. Solids **4**, 208 (1970).
[46]P. Debye, Polar Molecules (Dover, New York, 1945).
[47]H. Frohlich, *Theory of Dielectrics* (Clarendon, Oxford, 1949).
[48]K. Som, S. P. Sengupta, and B. K. Chaudhuri, Indian J. Phys. **62A**, 217 (1988).
[49]E. J. Osquiguil, L. Civale, R. Decca, and F. de la Cruz, Phys. Rev. B **38**, 2840 (1988).
[50]R. Manke and A. Molak, Solid State Commun. **66**, 1109 (1988).